Biochemical characterization of the mouse muscle-specific enolase: developmental changes in electrophoretic variants and selective binding to other proteins

Tatyana MERKULOVA, Marguerite LUCAS, Carole JABET, Noël LAMANDÉ, Jean-Denis ROUZEAU, François GROS, Monique LAZAR and Angélica KELLER*

Biochimie Cellulaire, CNRS UPR 9065, Collège de France, 11 place Marcelin Berthelot, 75231 Paris Cedex 05, France

The glycolytic enzyme enolase (EC 4.2.1.11) is active as dimers formed from three subunits encoded by different genes. The embryonic $\alpha\alpha$ isoform remains distributed in many adult cell types, whereas a transition towards $\beta\beta$ and $\gamma\gamma$ isoforms occurs in striated muscle cells and neurons respectively. It is not understood why enolase exhibits tissue-specific isoforms with very close functional properties. We approached this problem by the purification of native $\beta\beta$-enolase from mouse hindlimb muscles and by raising specific antibodies of high titre against this protein. These reagents have been useful in revealing a heterogeneity of the β-enolase subunit that changes with *in vivo* and *in vitro* maturation. A basic carboxypeptidase appears to be involved in generating an acidic β-enolase variant, and may regulate plasminogen binding by this subunit. We show for the first time that pure $\beta\beta$-enolase binds with high affinity the adjacent enzymes in the glycolytic pathway (pyruvate kinase and phosphoglycerate mutase), favouring the hypothesis that these three enzymes form a functional glycolytic segment. $\beta\beta$-Enolase binds with high affinity sarcomeric troponin but not actin and tropomyosin. Some of these binding properties are shared by the $\alpha\alpha$-isoenolase, which is also expressed in striated muscle, but not by the neuron-specific $\gamma\gamma$-enolase. These results support the idea that specific interactions with macromolecules will address muscle enolase isoforms at the subcellular site where ATP, produced through glycolysis, is most needed for contraction. Such a specific targeting could be modulated by post-translational modifications.

INTRODUCTION

In mammals, the glycolytic enzyme enolase (2-phospho-D-glycerate hydro-lyase; EC 4.2.1.11) is found as homodimers and heterodimers formed from three subunits α, β and γ, each encoded by one distinct gene [1,2]. During ontogenesis, the $\alpha\alpha$ embryonic isoform remains distributed in most adult cell types, whereas a transition towards specific isoforms occurs in two tissues with high and fluctuating energy requirements: $\alpha\gamma$ and $\gamma\gamma$ in the nervous system, $\alpha\beta$ and $\beta\beta$ in striated muscles [3–5]. It is noteworthy that, among glycolytic enzymes having isoforms with preferential expression in nervous or striated muscle tissues [6–8], the enolase isoenzyme family is unique for the strict cell-type specificity of the β and γ subunits.

We have previously established the profiles of α- and β-enolase transcripts and subunits during rodent striated muscle development. A decrease in α-enolase gene expression accompanies muscle maturation. At all stages of development, β-enolase gene expression is restricted to striated muscles. In the mouse embryo, β-enolase transcripts are detected in cardiac tube and newly formed myotomes. The gene is further up-regulated at various stages of muscle development, and appears to be under innervational and hormonal control [9–11]. At the adult stage, β-enolase transcript and subunit accumulate preferentially in fast-twitch fibres of hindlimb muscles, where the $\beta\beta$ isoenzyme accounts for more than 90% of total enolase activity [9,11–13].

As for many isoenzymes of the glycolytic pathway, it remains unclear why enolase exhibits isoforms with very close functional properties. Indeed, all three purified enolase homodimers ($\alpha\alpha$, $\beta\beta$ and $\gamma\gamma$) display similar kinetic parameters [14,15]. Sequence analyses from cloned cDNAs of various species and crystallographic studies with the pure yeast and lobster enolases [16,17] demonstrate that the enolase has maintained a highly conserved primary and tertiary structure throughout evolution. In mammals, there is 82% amino acid sequence identity between the three subunits. Interestingly, short variable regions characteristic of each subunit isoform are situated on the surface of the enolase molecule and are probable sites of contact with other macromolecules [16]. It was therefore tempting to speculate that enolase isoforms differ in their abilities to interact with cytoskeleton elements and/or other components of the cell. Previous observations suggest that glycolytic enzymes are involved in the formation of multiprotein complexes [18,19]. Thus in muscle cells, the structural characteristics of muscle-specific isoenzymes [20–22] would permit their accumulation near the muscle contractile apparatus, so that the ATP produced via glycolysis could be more efficiently delivered and used for contraction.

In order to assess this hypothesis in the case of enolase, we investigated whether the pure mouse $\beta\beta$-isoenolase could associate with other muscle proteins, such as glycolytic enzymes and cytoskeletal proteins. Modulations of such interactions by post-translational modifications of the β subunit could accom-

Abbreviations used: 2-PGA, 2-phospho-D-glycerate; PEP, phosphoenolpyruvate; MCK, muscle creatine kinase; DNP, dinitrophenol; NEpHGE, non-equilibrium pH gradient electrophoresis; PBSTG, 0.1% (v/v) Tween 20 in PBS containing 0.5% (w/v) gelatin; CPB, carboxypeptidase B; PK, pyruvate kinase; PGM, phosphoglycerate mutase.

* To whom correspondence should be addressed.

pany developmental changes in muscle energy metabolism. We have raised specific polyclonal antibodies by injection of native $\beta\beta$-enolase that had been purified from adult mouse limb muscles by a simple and original procedure. These reagents have been useful to reveal a microheterogeneity of the β-enolase subunit that changes with myogenic maturation. A specific carboxypeptidase appears to be involved in generating the acidic β-enolase variant. Furthermore, we demonstrate that pure mouse $\beta\beta$-enolase binds with high affinity other muscle enzymes important for energy metabolism. The ubiquitous $\alpha\alpha$ isoform shares some of these binding properties which, however, are never observed with the neuron-specific $\gamma\gamma$ isoform of enolase. We also show that only $\beta\beta$-isoenolase binds with high affinity sarcomeric troponin. None of the studied isoforms of enolase binds actin or tropomyosin.

MATERIALS AND METHODS

Protein extracts

Mice of the OF1 strain (IFFA CREDO) were killed by cervical dislocation. Hindlimb muscles, dissected from embryonic day 15 (E15) mice to the adult stage (70 days postnatally: P70), were quickly frozen in liquid nitrogen and stored at -80 °C. Frozen tissue samples were dropped in cold extraction buffer and quickly treated with a Polytron homogenizer. Extraction buffer was always 15 mM sodium phosphate buffer, pH 7.2 (5 ml of buffer per g of tissue), containing 4 mM magnesium acetate and a proteinase inhibitor, aprotinin, as indicated by the manufacturer (Boehringer Mannheim, Meylan, France). The supernatant obtained from a low-speed centrifugation (1500 ***g***, 15 min) was centrifuged for 90 min at 100000 ***g***. Aliquots were kept frozen at -20 °C until further use. Extracts were also prepared from the embryonic fibroblast cell line C3H $10T^{1/2}$, and from myoblasts or myotubes obtained by cultivating the myogenic C2.7 cell line as previously described [23]. Protein concentration was determined by the method of Bradford [24], using BSA as a standard.

Enolase enzyme assays

Enolase assays were performed at 30 °C. Activity was measured spectrophotometrically at 240 nm as the conversion of sodium 2-phospho-D-glycerate (2-PGA) into phosphoenolpyruvate (PEP) and expressed in International Units (IU) as previously described [14].

Enolase purification

Following homogenization of 100 g of hindlimb muscles, cell debris was removed by centrifugation in a Sorvall (5000 ***g***, 15 min), and the supernatant submitted to high-speed centrifugation (90 min at 100000 ***g***). Whereas the $\alpha\alpha$-enolase is precipitated between 40 and 60 % ammonium sulphate saturation, the muscle-specific enolase is recovered between 60 and 80 % ammonium sulphate [14]. This pellet (P60-80), containing muscle-specific enolase activity (mostly $\beta\beta$), was resuspended in the extraction buffer described above, dialysed against large volumes of 15 mM Tris/HCl buffer, pH 9.0, containing 4 mM magnesium acetate, and chromatographed on a DEAE–Sepharose column (4 cm × 34 cm). Bound proteins were eluted with a stepwise pH gradient of 15 mM Tris/HCl (pH 9.0 to 7.0, with 0.5 pH unit per step). Each fraction was analysed for enolase activity and protein content (A_{280}). Fractions with highest specific activities were pooled, brought to 30 % ammonium sulphate saturation and subjected to a second chromatography on a phenyl-Sepharose column (2.5 cm × 5.5 cm) using a stepwise ammonium sulphate gradient (30 % to 0 %, with 10 % per step). The collected enolase peak could be chromatographed on a second DEAE–Sepharose column (2.5 cm × 4.5 cm), resulting in a further increase in specific activity. Pure mouse $\alpha\alpha$- and $\gamma\gamma$-enolase isoforms were prepared from brain, as previously described [14].

Immunological reagents

Antibodies directed against pure rabbit muscle creatine kinase (MCK) were produced in chicken and were kindly given by Georges Foucault and Monique Vacher, Laboratoire de Biologie Physicochimique, Orsay, France.

Production of specific antibodies directed against the commercially available rabbit β-enolase in sheep [9] and against mouse α- and γ-enolase in rabbit [14] has been previously described. For Western blot studies, the anti-MCK serum was diluted 1/250 and the anti-α and -γ-enolase sera were diluted respectively 1/5000 and 1/1000. The anti-β-enolase serum was affinity-purified and used at the dilution 1/300 [10]. Peroxidase-coupled secondary antibody was anti-goat IgG in the case of β-enolase, anti-rabbit IgG in the case of α- and γ-enolase and anti-chicken IgG in the case of MCK (BIOSYS, Compiègne, France).

New anti-β-enolase sera were produced in two rabbits by several 300 μg monthly injections of the purest mouse $\beta\beta$-enolase fractions obtained as described in the present report. In an effort to induce a stronger immunological response, the pure enzyme preparation was modified by dinitrophenol (DNP) coupling [25] before injection into two other rabbits. No significant difference was observed between animals injected with native or DNP-modified enzyme.

Gel electrophoresis and Western blot analysis

Analytical SDS/PAGE was conducted using the Hoeffer miniature slab gel electrophoresis unit followed by Western blot analyses, as previously described [11].

Two-dimensional gel electrophoresis was performed as described by O'Farrell, with minor modifications [26]. Briefly, in the first dimension, protein samples were submitted to a basic non-equilibrium pH gradient electrophoresis (NEpHGE) in 4 % (w/v) polyacrylamide gels containing 2 % (w/v) Ampholines (pH 3.5–10.0), for 5 h at 500 V. For the second dimension, electrophoresis was run overnight in the presence of 0.1 % (w/v) SDS, in 8 % polyacrylamide gels (acrylamide/bisacrylamide ratio 1:40) with 10 mA per slab gel. The gels were then either silver stained [27] or electrically transferred on to Hybond C membranes (Amersham). The Western blots thus obtained were kept dry until immunological treatments were performed following the protocol indicated by Amersham for the enhanced chemiluminescence Western blotting detection system.

The first dimension NEpHGE was also used for pI determination of purified proteins. In this case, the gels were stained with Coomassie Blue R 250 and the pI of the individual protein subspecies determined as a function of their migration, using commercially available proteins of known pI as standards.

ELISA

ELISA 96-well microtitration plates (Nunc immunoplates from Polylabo Paul Block) were coated with varying amounts of tissue extracts or purified mouse $\beta\beta$-enolase in PBS (10 mM NaCl in 0.1 M phosphate buffer, pH 7.4) overnight at 4 °C, then overcoated with 100 μl of 1 % (w/v) gelatin in PBS for 1 h at 37 °C and washed three times with large amounts of 0.1 % (v/v) Tween 20 in PBS. Except for washes, volumes of various reagents added to the wells in the following steps were always

50 μl. Plates were incubated for 2 h at 37 °C with immune serum diluted in PBST containing 0.5 % gelatin (PBSTG) and washed four times as before. They were then incubated for 2 h at 37 °C with β-galactosidase-labelled antibody directed against rabbit IgG (dilution 1:1500 in PBSTG). After washing as above, β-galactosidase activity was determined by adding freshly prepared substrate solution [1 mg/ml *ortho*-nitrophenyl β-D-galactopyranoside dissolved in PBS, containing 1 % (v/v) β-mercaptoethanol]. Following 15–30 min incubation at 37 °C, the reaction was stopped with 0.5 M Na_2CO_3 and the absorbance at 405 nm read in an MR 580 Microelisa Auto Reader (Dynatech Instruments Inc.).

A similar ELISA procedure was used for studies of enolase interaction with other proteins. In this case, the microtitre plate was coated with the analysed ligand (0. 5 μg per well), overcoated with 2 % (w/v) BSA in PBS and incubated with serial dilutions of pure $\beta\beta$-enolase in PBSTG for 2 h at 37 ° C, at three different pH values (6.5, 7.0 and 7.4). The plate was then sequentially incubated with the anti-β-enolase serum R2 selected for these studies (see the Results section) diluted 1/1000 and with the enzyme–antibody conjugate and substrate, as described above. Background values of A_{405}, obtained when the plates were coated with BSA instead of the studied ligand, were always deducted from values obtained in the assay.

Other reagents

Plasminogen, carboxypeptidase B (CPB), benzylsuccinic acid, pI standards and pure proteins used in binding assays were from Sigma. The specific Plummer's inhibitor of CPB and N [28,29], DL-2-mercaptomethyl-3-guanidino ethylthiopropanoic acid (Mergetpa) was from Calbiochem (La Jolla, CA, U.S.A.). All other materials were of analytical reagent grade.

Computer analysis

Sequences were analysed and theoretical pI values computed using the programs available on B.I.S.A.N.C.E (CITI2; [30]).

RESULTS

Purification of muscle-specific enolase from adult mouse hindlimb

A typical purification is shown in Table 1, starting with 100 g of mouse hindlimb muscle. All enolase activity binds to the DEAE–Sepharose column at pH 9.0 and is eluted from the column at pH 8.5 in one peak (DEAE–Sepharose-1) (Figure 1). The efficiency of the DEAE chromatography step is evident from SDS/PAGE analysis (Figure 2A), comparing lane 1 (P60-80) with lane 2 (eluted peak at pH 8.5). The latter fraction contains a major polypeptide of size 46 ± 1 kDa (mean $\pm$ S.D. from $n = 6$ independent measurements), which is the only one detected in the final enzyme preparation (lane 3), obtained after two more chromatographic steps with a phenyl-Sepharose column and a DEAE–Sepharose column (Table 1). This pure enzyme preparation (Figure 2A, lane 3), with a specific activity reaching 83 units/mg of protein, was used for Michaelis constant determinations as previously described [14], giving the K_m value $7.8(\pm 1.1) \times 10^{-5}$ M (mean $\pm$ S.D., $n = 4$) for 2-PGA. The purified enzyme has been stored at -74 °C in elution buffer at pH 7.0 for up to 10 months with no apparent loss of activity, provided that multiple freezing and thawing steps are avoided. Western blot analysis demonstrates that the purified mouse $\beta\beta$-enolase gives a

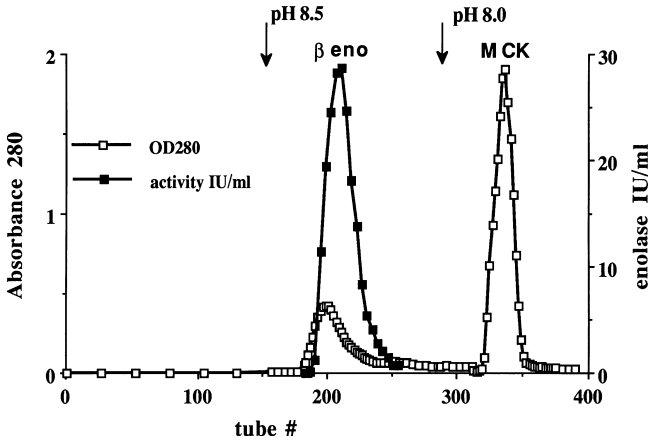

Figure 1 Elution profile of the first DEAE–Sepharose column

Elution of the column was performed as described in the Materials and methods section. Enolase activity and protein content were measured in the 5 ml fractions. β eno = β-enolase; OD = absorbance; IU/ml = units/ml; tube # = tube number.

Table 1 Example of a purification of $\beta\beta$-enolase from mouse hindlimb muscle

Besides removing $\alpha\alpha$-enolase from the high-speed supernatant (HSS; see the Materials and methods section), the ammonium sulphate precipitation step yields a nearly two-fold increase in specific activity. Although most of the enolase activity is recovered from the 60–80% ammonium sulphate precipitation step when assayed immediately after dissolving the pellet (P60-80.1), approx. 25% of the total activity has been lost from the same sample assayed just before application to the next chromatographic step (P60-80.2) without a significant change in specific activity, whether kept in extraction buffer (pH 7.2) or dialysed against buffer at pH 9.0. Enolase activity binding to the DEAE–Sepharose column at pH 9.0 is eluted from the column at pH 8.5 in one peak (DEAE–Sepharose-1), with an overall recovery of 30%. Further elution with a pH gradient between 8.5 and 7.0 does not reveal any fraction with enolase activity. Most of the recovered enolase activity is eluted by using 10% ammonium sulphate from the phenyl-Sepharose column. Rechromatography on a second DEAE–Sepharose column yields one enolase peak (DEAE–Sepharose-2) with higher specific activity.

Fractions	Total protein (mg)	Total activity (units)	Specific activity (units/mg)	Yield (%)
HSS	4235	25818	6.1	100
P60-80.1	2257	23947	10.6	92.8
P60-80.2	1707	17366	10.2	67.3
DEAE–Sepharose-1 (pH 8.5)	94	5122	54.5	19.8
Phenyl-Sepharose [10% $(NH_4)_2SO_4$]	31	2016	65	7.8
DEAE–Sepharose-2 (pH 8.5)	15	1245	83	4.8

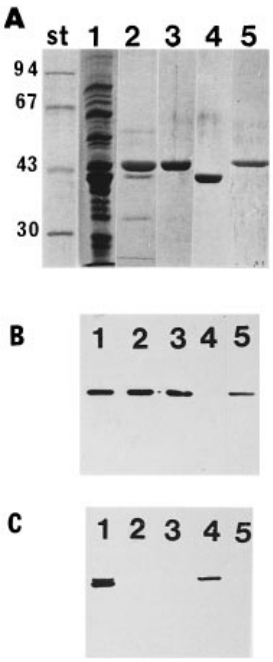

Figure 2 Analysis by SDS/PAGE and Western blotting of various fractions obtained during the purification procedure

(**A**) Coomassie Blue staining. 1, P60-80 (16 μg); 2, aliquot of the peak eluted at pH 8.5 from DEAE–Sepharose-1 (3 μg); 3, aliquot of the enolase activity peak eluted at pH 8.5 from DEAE–Sepharose-2 (2 μg); 4, aliquot of the protein peak eluted at pH 8.0 from DEAE–Sepharose-1 (2 μg); 5, aliquot of the protein peak eluted at high salt from DEAE–Sepharose-2 (2 μg). Molecular-mass markers (kDa) are indicated on the left. (**B**) and (**C**) Western blots of gels similar to (**A**), but with smaller amounts of proteins in the applied fractions: 1, 0.5 μg; 2–5, 0.2 μg. Blots were revealed using the enhanced chemiluminescence blotting detection system (see the Materials and methods section) with the following primary antibodies: anti-rabbit β-enolase serum (**B**); anti-rabbit MCK serum (**C**).

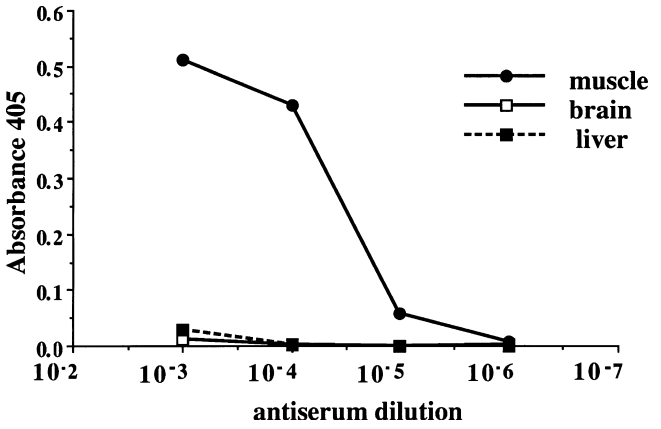

Figure 3 Specificity of the R2 antiserum produced against pure mouse $\beta\beta$-enolase

Wells of the ELISA plates, coated with 2 μg of various mouse tissue extracts, were incubated with serial dilutions of the anti-mouse β-enolase serum R2 (50 μl). Immunological reaction was monitored by measuring the absorbance at 405 nm, which is indicative of the β-galactosidase activity coupled to the secondary antibody (see the Materials and methods section).

strong reaction with the sheep anti-β-enolase antibodies previously obtained in our laboratory (Figure 2B, lane 3).

Further elution of the second DEAE–Sepharose column with high salt resulted in the recovery of a single 46 kDa polypeptide reacting with anti-β-enolase antibodies in Western blot (Figures 2A and 2B, lane 5) but devoid of any enolase activity.

Surprisingly, the prominent protein peak eluted from the first DEAE–Sepharose column at pH 8.0 (Figure 1) contained only one polypeptide of size 41 ± 1 kDa (mean $\pm$ S.D., $n = 4$) (Figure 2A, lane 4). These features suggested that this could be the muscle-specific isoform of creatine kinase (MCK), which was confirmed by activity measurements (Dr. M. Arrio-Dupont, Orsay, France) and reactivity with anti-MCK-specific antibodies (Figure 2C, lane 4).

Characterization of polyclonal antibodies raised against mouse $\beta\beta$-enolase

In order to generate polyclonal antibodies of high titre directed against the muscle-specific enolase isoform, rabbits were injected with aliquots of the purest mouse $\beta\beta$-enolase fraction (see Table 1 and Figure 2, lane 3). Figure 3 shows a typical set of ELISA titration curves obtained with one of the most sensitive anti-β-enolase sera (R2), demonstrating a reaction only with extracts from striated muscles and not with those from liver (expressing only the $\alpha\alpha$-enolase isoform) or brain (containing the $\alpha\alpha$-, $\alpha\gamma$- and $\gamma\gamma$-enolase). This antiserum allows the detection of 1 ng of pure enolase in similar titration experiments, with pure mouse $\beta\beta$-enolase bound to the wells instead of tissue extracts. Addition of pure muscle enolase, but not BSA, to the antiserum strongly decreases the absorbance in this ELISA test (results not shown). Western blot analyses of liver, brain and muscle extracts, similar to those shown in Figure 2(B), indicate that the newly produced antisera are specific for the β-enolase subunit. They are of higher titre than the serum previously obtained by injecting sheep with the commercially available rabbit $\beta\beta$-enolase, which should be used at a dilution of 1/300 in this test; whereas, the R2 serum gives similar results at a dilution of 1/50000.

Antisera generated against the mouse muscle isoenolase allow the specific detection of the β subunit in extracts from other species (rat, rabbit and human), although less diluted serum should be used for recognizing the human β-enolase subunit (results not shown).

Evidence for heterogeneity of the mouse β-enolase subunit

Adult striated muscle extracts were analysed by two-dimensional gel electrophoresis followed by silver staining (Figure 4A). Comparison with a Western blot obtained from a similar gel, after incubation of the membrane with the R2 antiserum (Figure 4B), allows identification of a heterogeneous protein spot (Figure 4A, arrows) as the β-enolase subunit, no other protein spot being detected by this antiserum. The β-enolase subunit is resolved into two major subspecies of the same apparent molecular mass. The relative intensity of these two spots could vary from extract to extract, the more basic spot being usually the most abundant. The heterogeneity pattern of the purified mouse β-enolase (Figure 4D) is very similar to that of β-enolase contained in adult muscle extracts (Figure 4B). Under these migration conditions, the mouse MCK is also resolved into two major isoproteins (Figure 4C, M), as has been described in the case of other species [31].

In order to analyse any modification in the microheterogeneity of the β-enolase subunit during differentiation or following biochemical treatments (see below), it was necessary to compare the position of each spot on the Western blot obtained following

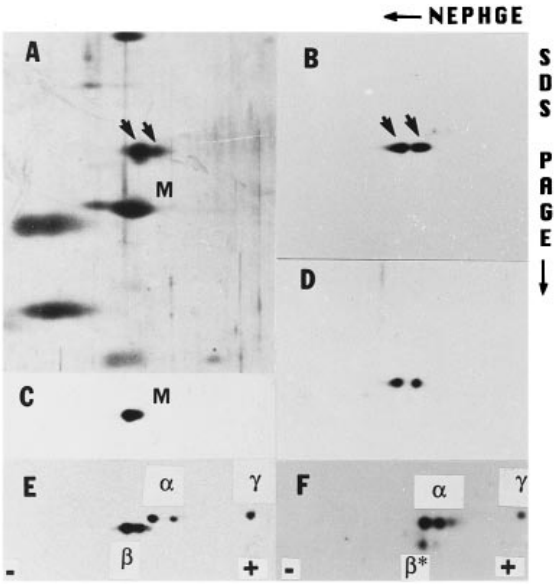

Figure 4 Two-dimensional gel electrophoresis and Western blot analyses reveal heterogeneity of the mouse β-enolase subunit

(**A**) Hindlimb muscle extract (5 μg); the gel was silver stained. (**B**) to (**F**) Western blot analysis following two-dimensional gel electrophoresis. (**B**) and (**C**) Hindlimb muscle extract (2 μg); the blots were revealed with the R2 anti-mouse β-enolase serum (**B**) and the anti-rabbit MCK serum (**C**). (**D**) Pure mouse β-enolase (50 ng) revealed with the R2 serum. In (**E**) and (**F**) the blots were revealed sequentially by the three antisera directed against α-, β- and γ-enolase subunits. (**E**) β-Enolase (80 ng) plus mouse brain extract (7.5 μg). (**F**) Inactive β-enolase (1 μg; see Figure 2, lane 5) plus mouse brain extract (2 μg). β^* indicates the main spot of inactive β-enolase. Note that (**F**) has been overexposed compared with (**E**). + and - indicate the direction of protein migration during NEpHGE (NEPHGE).

Table 2 pI values of mouse enolase subunits; comparison with expected values

The pure proteins were submitted to electrophoresis in the first dimension (NEpHGE) only. Gels were stained with Coomassie Blue and the pI of individual protein subspecies determined as a function of their migration, using commercially available proteins of known pI as standards. The pI values of the α- and γ-enolase subunits from mouse brain extracts were measured by comparison with the migration of the MCK and the β-enolase subunit in two-dimensional gel electrophoresis. Results are means $\pm$ S.E.M., with n indicating the number of determinations. Expected pI values were obtained from computer analysis.

Enolase subunit	n	pI $\pm$ S.E.M.	Expected pI value
Mouse enolase			
α1	6	6.51 $\pm$ 0.02	7.07
α2	6	6.32 $\pm$ 0.03	
α3	6	6.20 $\pm$ 0.00	
α4	1	6.10	
β1	3	6.74 $\pm$ 0.05	7.45
β2	3	6.61 $\pm$ 0.01	
γ	6	5.39 $\pm$ 0.05	5.2
Rabbit enolase			
β1	3	8.05 $\pm$ 1.29	8.2
β2	3	7.3 $\pm$ 0.56	

two-dimensional gel electrophoresis with protein markers. As the α- and γ-enolase subunits can be detected with specific antibodies and used as references, it appeared most convenient to add a constant amount of mouse brain extract to the analysed samples, just before electrophoresis (Figure 4E). We observe that the brain α-enolase is separated into several variants, with up to four spots visible upon overexposure (see Table 2). Under these migration conditions, the neuron-specific γ subunit appears as one most acidic spot.

The pI of each variant of the pure β-enolase was estimated by comparing their migration in the first dimension (NEpHGE) with that of commercial markers (Table 2). In the same way, pIs of the two spots corresponding to the mouse MCK were measured (pI: 6.73 $\pm$ 0.13 and 6.84 $\pm$ 0.21, $n = 4$), as well as pIs of the cerebral α- and γ-enolase subunits. The mouse β-enolase subunit is the most basic mouse enolase isoform, its most acidic variant (β2: pI = 6.6) migrating close to the most basic α-enolase variant (α1: pI = 6.5).

We also analysed the protein obtained by high-salt elution from the second DEAE–Sepharose column (Figure 2A, lane 5), that is recognized by the anti-β-enolase sera (Figure 2B, lane 5) but lacks enolase activity, and could thus represent an inactivated form of the β-enolase subunit. Comparison with the most basic cerebral α-enolase variant (Figure 4F) shows that, in this sample, the main β-enolase spot (β^*) is more acidic than the two β-enolase variants usually found in muscle extracts. It also appears to be of smaller size and is most probably a proteolytic product formed despite the addition of aprotinin in the extraction buffer.

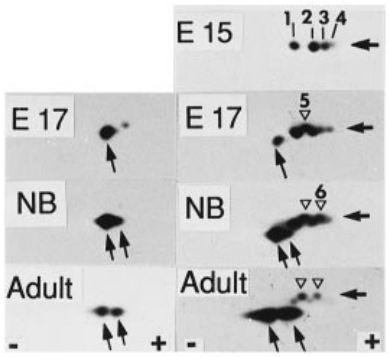

Figure 5 Changes in the microheterogeneity of α-and β-enolase subunits during mouse striated muscle development

For Western blot analysis, 20 μg hindlimb muscle extracts were used. (Left): blots were revealed with the anti-β-enolase serum (R2). They were then treated with the anti-α-enolase serum (right). Oblique arrows, β-enolase; horizontal arrows, α-enolase; open arrowheads, slow variants of α subunit. E15 (embryonic day 15): four variants of the α subunit are visible, numbered 1 to 4; the β-enolase subunit is barely detectable upon longer exposure times and is not shown here on the left panel. E17 (embryonic day 17): on the left panel, because of the high level of the α subunit, following incubation with the anti-β-enolase serum alone, the most basic α-enolase variant (1) is detected as one spot of larger size at the right of the arrow; on the right panel, one slow variant of α subunit (5) is already visible. NB: newborn; a second slow variant of α subunit (6) is now visible. Adult: note that the blot on the right panel has been overexposed in order to reveal the α-enolase subunit.

Changes in α- and β-enolase electrophoretic variants during *in vivo* and *in vitro* myogenic maturation

The pattern of α and β subunit microheterogeneity in hindlimb muscle extracts was examined in mice, from E15 to the adult stage (P70). Western blots were sequentially reacted with the anti-β-enolase serum (Figure 5, left panel) and with the anti-α-enolase serum (Figure 5, right panel). In the less mature muscles (E15), a large amount of the ubiquitous α subunit is visible as four spots comparable with those of the adult brain (see α in

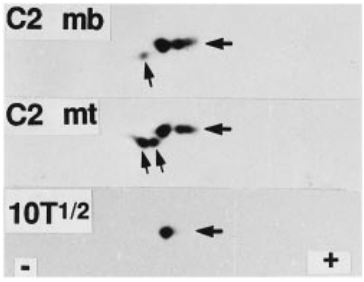

Figure 6 Microheterogeneity of β-enolase subunit in mouse cultured cells

Extracts (30 μg) were prepared from cell lines. C2.7 cells were harvested at the myoblast stage (C2 mb) or after 72 h in differentiation medium, at the myotube stage (C2 mt). The $10T^{1/2}$ fibroblast cell line was used as a control. Blots were incubated with both anti-β- and anti-α-enolase serum. Oblique arrows, β-enolase; horizontal arrows, α-enolase.

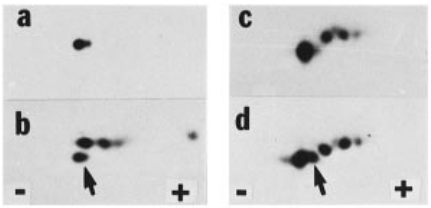

Figure 7 Modifications of β-enolase microheterogeneity by CPB and the specific inhibitor Mergetpa

Western blot analysis was conducted as described in the Materials and methods section, and in the legend to Figure 5, to reveal both the β-enolase subunit and the brain α-enolase added to samples as a reference. (Left): (**a**) pure β-enolase (50 ng) was treated with CPB (20 units) for 2 h at 25 °C; (**b**) 7.5 μg of brain extract was added to a sample identical with that shown in (**a**). (Right): hindlimb muscle extracts (2 μg) were analysed in the presence of 2 μg of brain extract; (**c**) the extract was prepared in the presence of the specific basic carboxypeptidase inhibitor, Mergetpa (40 μM); (**d**) control extract was prepared as usual (see the Materials and methods section). The arrow points to the most acidic variant of the β-enolase subunit.

Figure 4F and Table 2), with the minor most acidic spot (α4) visible only following longer exposure times. In contrast, the β-enolase subunit is expressed as one faint spot at E15 (results not shown). The large increase in concentration of β-enolase subunit occurring between E15 and E17 allows easy detection at this later time (Figure 5, E17). Comparison with the migration of the α-enolase variants shows that it corresponds to the most basic β-enolase variant of adult extracts. At this stage (E17), the acidic variant just becomes visible and further accumulates with maturation (Figure 5, newborn; NB). By P5, the pattern of β subunit microheterogeneity has not changed and the α-enolase subunit level has decreased (results not shown). The pattern characteristic of the adult β-enolase (Figure 5, Adult), with two variants, is reached by P21.

The pattern of muscle α subunit heterogeneity also changes with maturation. All four detectable α subunit spots of embryonic muscle (E15), adult brain (Figure 4F and Table 2) or liver (results not shown) have the same apparent molecular mass, while those of muscle include two spots migrating less rapidly. Comparison of Western blots obtained from adult muscle extracts with Western blots obtained by mixing together brain and muscle extracts before electrophoresis reveals that the two muscle α-enolase spots, which move slightly ahead (smaller apparent size), perfectly superimpose the two most basic spots (α1 and α2) of brain α-enolase. Thus the two spots of larger size (open arrowheads indicating α5 and α6 in Figure 5) could represent α-enolase variants specific for muscle. At E17, the basic spot of the α-enolase slow doublet (α5, open arrowhead) is already visible; the acidic spot (α6, open arrowhead) becomes visible in newborn extracts where the four detectable α-enolase variants are similar to those present in adult muscle extracts. In all tested adult muscle tissues (heart, gastrocnemius, soleus) the most basic α-enolase subspecies (α1) is the most abundant variant (results not shown).

Changes in the pattern of β subunit microheterogeneity are also observed during myogenesis *in vitro*. We have previously shown that the β-enolase gene is already expressed in C2.7 cells at the myoblast stage, and is up-regulated during differentiation [32]. Extracts of these cells were examined at the myoblast stage and in myotubes collected after 72 h in differentiation medium (Figure 6). It is possible to compare β subunit migration with that of the endogenous α subunit, which remains at a high enough level in myotubes. At the myoblast stage, only the most basic β subunit variant is detected. Two β variants, similar to those observed in adult striated muscles, are visible in differentiated C2.7 myotubes. In the fibroblast cell line $10T^{1/2}$, only the α-enolase subunit is detected as the most basic variant.

Removal of C-terminal lysine partially accounts for the microheterogeneity of the β-enolase subunit

The observed β subunit variants, of identical apparent molecular mass, are most probably generated by post-translational modifications. Phosphorylation could account for the production of acidic variants. To test this hypothesis, purified $\beta\beta$-enolase was treated with increasing concentrations (up to 100 units/ml) of either alkaline or acid phosphatase, and then submitted to two-dimensional gel electrophoresis and Western blot analysis. Using α and γ subunits as internal markers, no difference was found in the mobilities and relative intensities of the two major variants of control or treated β-enolase subunit. Similarly, no difference was observed in the pattern of β-enolase microheterogeneity of muscle extracts prepared as usual (Figure 4B), or of extracts prepared in the presence of a large excess of 3-phospho-D-glycerate (20 mM) added as competitive substrate to neutralize the action of cellular phosphatases. Finally, monoclonal antibodies directed against phosphoserine, phosphothreonine or phosphotyrosine did not reveal any specific reaction with any of the β-enolase spots shown on Western blots (results not shown).

The amino acid sequence of all mammalian α- and β-enolase subunits are characterized by a C-terminal lysine [16] that could be removed by a specific basic carboxypeptidase. When the purified enzyme is incubated with increasing concentrations of the commercially available CPB, we observe the disappearance of the most basic variant (Figures 7a and 7b) compared with the untreated β subunit (Figure 4E), which is consistent with the elimination of a basic amino acid. A concentration of 2 units/ml CPB is sufficient to transform completely 1 mg/ml of pure β-enolase into its more acidic form. Increasing the CPB concentration up to 100 units/ml with a concomitant extension of the incubation time from 2 to 24 h did not generate any additional variant. When muscle extracts are prepared in the presence of Mergetpa, a specific inhibitor of CPB [28,29], we observe a redistribution of the β-enolase variants towards the more basic direction, so that the most acidic spot becomes almost undetectable (Figure 7c). A similar result was obtained using another inhibitor, benzylsuccinic acid (results not shown). When modified and control $\beta\beta$-enolases were examined for their abilities to

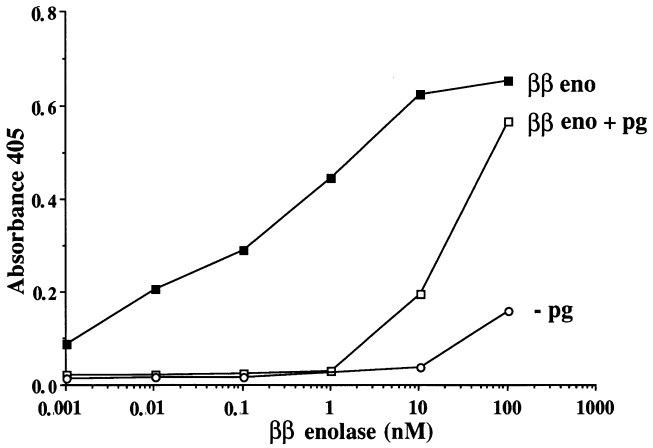

Figure 8 Binding of $\beta\beta$-enolase ($\beta\beta$ eno) to plasminogen

Wells of the ELISA plates, coated with 0.5 μg of plasminogen (pg), were incubated with serial dilutions of the pure mouse $\beta\beta$-enolase for 1 h at 37 °C, followed by incubation with the R2 serum and further processing for an ELISA assay as described in the legend to Figure 3 and in the Materials and methods section.

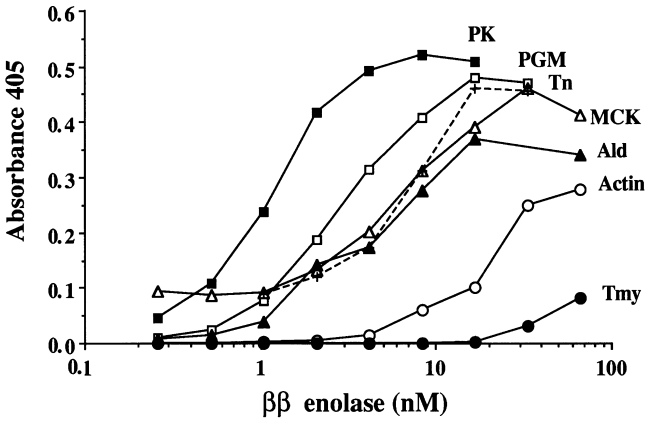

Figure 9 $\beta\beta$-enolase interaction with various muscle proteins at pH 6.5

Details as described in Figure 8 legend, except that wells were coated with 0.5 μg of the various studied proteins and the incubation time with the pure $\beta\beta$-enolase was 2 h. Ald, aldolase; Tmy, tropomyosin; Tn (–––), troponin.

Table 3 Binding of $\alpha\alpha$- and $\beta\beta$-enolase to various ligands at two pH values

Binding of the pure mouse $\alpha\alpha$- and $\beta\beta$-enolase to various ligands was studied as described in the Materials and methods section and in the legends to Figures 8 and 9. The EC_{50} values correspond to the concentrations of pure enolase necessary to reach half-maximal binding. The values shown here were computed from curves as shown on Figures 8 and 9. Duplicate experiments yielded nearly identical results.

	EC_{50} (nM)			
	$\alpha\alpha$		$\beta\beta$	
pH ...	6.5	7.4	6.5	7.4
Plasminogen	0.1	0.1	0.1	0.1
PK	2.0	4.5	1.0	7.0
PGM	1.5	2.5	3.0	8.0
MCK	1.8	3.0	5.0	7.0
Aldolase	2.0	4.0	6.0	25
Troponin	20	18	4.0	8.0

catalyse the conversion from 2-PGA into PEP, no difference in kinetic parameters was observed.

Mouse $\beta\beta$-enolase specifically binds plasminogen

In a search to characterize plasminogen binding sites, a major protein was recovered from membrane preparations of the human mononucleated U937 cell line and identified as α-enolase [33]. It was further demonstrated that the properties of a plasminogen receptor were mostly linked to the last 16 amino acids of the C-terminal sequence of the α-enolase subunit. In mammals, the C-terminal sequence of the β- but not the γ-enolase subunit is similar to that of the α-enolase [16]. Further evidence indicates that the β [34], but not the γ subunit [35], could also have the properties of a plasminogen receptor. We investigated whether purified mouse $\beta\beta$-enolase could specifically bind plasminogen by means of a modified ELISA test. In this way a dose-dependent and saturable binding of $\beta\beta$-enolase to plasminogen was observed (Figure 8). Saturation of binding to plasminogen is reached with 10 nM $\beta\beta$-enolase. The concentration of $\beta\beta$-enolase necessary to achieve its EC_{50} is an indication of its affinity for plasminogen, and is found here to be in the region of 0.1 nM. A similar result was obtained using commercial rabbit $\beta\beta$-enolase. The binding of $\beta\beta$-enolase to plasminogen is inhibited by 1 μM free plasminogen added to the microtitre wells, at the same time as the enolase (Figure 8). No significant binding is observed to wells that have not been coated with plasminogen. The $\beta\beta$-enolase treated with CPB (100 units/ml, 24 h at 25 °C) does not bind significantly to plasminogen any longer (results not shown). Using similar ELISA tests, we have shown that pure mouse $\alpha\alpha$-enolase specifically binds plasminogen (Table 3), whereas the $\gamma\gamma$-isoenolase does not.

Interactions between mouse $\beta\beta$-enolase and various muscle proteins

Association of glycolytic enzymes into multiprotein complexes has been described in various cell types, and numerous studies have stressed the importance of such reversible, pH-dependent associations in controlling the efficiency of glycolysis [20,36,37]. We analysed the binding of pure mouse $\beta\beta$-enolase with the following commercially available glycolytic enzymes purified from rabbit muscle: pyruvate kinase (PK) and phosphoglycerate mutase (PGM), which are adjacent to enolase in the pathway, and aldolase, which is known to associate with cytoskeletal proteins. The interaction was studied at pH 7.4 and at two more acidic pH values, 7.0 and 6.5. At all pH values, a significant and saturable binding of $\beta\beta$-enolase to PK, PGM and aldolase was observed, as shown for pH 6.5 in Figure 9. Similarly, specific binding of $\beta\beta$-enolase to the mouse MCK purified in this study occurs. Binding to the sarcomeric proteins actin and tropomyosin is low and non-saturable, and should be considered to be non-specific (Figure 9). However, we observed a specific binding to muscle troponin. In all cases, binding affinities of mouse $\beta\beta$-enolase were higher at pH 6.5 than at pH 7.4, as indicated by lower EC_{50} values (Table 3). Results obtained at pH 7.0 and 6.5 were not significantly different. We find that the $\alpha\alpha$-enolase also

binds with high affinity PK, PGM, aldolase and MCK. In most cases, EC_{50} values obtained with $\alpha\alpha$- and $\beta\beta$-enolase are quite similar. However, at pH 7.4, $\alpha\alpha$-enolase binds aldolase with higher affinity than does $\beta\beta$-enolase. Interestingly, at all tested pH values, $\alpha\alpha$-enolase binds troponin with lower affinity than the muscle-specific isoform $\beta\beta$. In contrast, no significant binding of the neuron-specific $\gamma\gamma$-enolase to any of these muscle proteins was observed.

DISCUSSION

We have devised a simple and rapid method of purifying the muscle-specific isoform of enolase from adult mouse hindlimb muscle, which allows us to obtain large amounts of this enzyme without including the denaturing steps (heating, acetone-dried powder) classically used for this purification [15,38,39]. A further advantage of this method is that it also yields large quantities of another enzyme very important in energy metabolism, the muscle-specific creatine kinase. The specific activity of pure mouse $\beta\beta$-enolase, as well as the K_m of the enzyme for the substrate (2-PGA), are comparable with values reported for this protein purified from other species [15,38,39], and the K_m value found here for $\beta\beta$-enolase is similar to that obtained for the other $\alpha\alpha$- and $\gamma\gamma$-enolase mouse isoforms [14]. Injection of the pure $\beta\beta$-enolase resulted in the production of antisera of high titre, specifically recognizing the β-enolase subunit of mouse and of the various tested species (human, rat, rabbit).

Changes in α- and β-enolase microheterogeneity accompany myogenic maturation

Analyses by two-dimensional gel electrophoresis and Western blotting reveal a heterogeneity of α- and β-enolase subunits. The existence of electrophoretic variants has already been reported for the purified rabbit β-enolase [38] and for the α-enolase present in mouse macrophages [40]. We find that the endogenous β-enolase subunit obtained from various adult mouse muscle extracts (heart, gastrocnemius and soleus muscles) always exhibits the same heterogeneous pattern, with two variants of identical size. It should be noted that each of the two variants of the β subunit could probably be subdivided in the gel electrophoresis into at least two other spots. In some extracts of dissected individual adult muscles, such additional spots are readily visible (results not shown). The nature of this additional heterogeneity is still under investigation. In extracts from foetal hindlimb muscles, only the most basic variant is visible, the most acidic variant becoming clearly visible by E19. A similar transition towards this more complex adult pattern is observed during the *in vitro* maturation of the myogenic C2.7 cells.

In extracts of immature muscles (E15) as well as of cultured myoblasts, the α subunit represents the major enolase isoform and exhibits up to four detectable electrophoretic variants. These variants are of identical size in brain and immature muscle. The characteristic pattern of adult muscle α subunit heterogeneity, with two variants of larger apparent size, is reached soon after birth and is also sometimes visible in C2.7 myotube extracts (results not shown). However, only the most basic variant of the α-enolase subunit is observed in extracts of the fibroblast cell line $10T^{1/2}$. These observations *in vivo* and *in vitro* suggest that different post-translational modifications may occur in different cell types, resulting in different α-enolase subunit variants.

Results of the developmental study *in vivo* show that the establishment of muscle-type heterogeneity for both the α and β subunits takes place during mouse muscle maturation, between E17 and birth, at the time of secondary fibre formation.

Search for post-translational modifications accounting for β-enolase microheterogeneity

The expected pI value from sequence data for the mouse β-enolase (7.45) is clearly more basic than that found experimentally (6.74 and 6.61). As values obtained here for the mouse γ-enolase and for the rabbit β-enolase are very close to the theoretical values (Table 2), this discrepancy does not appear to be a consequence of the pI determination procedure. From studies with the cloned human β-enolase gene, the only reported alternative splicing [41] does not modify the coding sequence. We therefore looked for post-translational modifications that could account for the observed β subunit variants.

The mouse β-enolase sequence exhibits several putative phosphorylation sites. Some of them, but not all, are common to the different isoforms (N. Lamandé, unpublished work). It is known that rabbit β-enolase is phosphorylated *in vitro* by protein kinase C [42]. However, our preliminary attempts to demonstrate a role for phosphorylation reactions in generating the β-enolase variants observed in muscle extracts were unsuccessful, possibly because of the low proportion of phosphorylated enolase in the extracts. In the case of the α subunit, phosphorylation has been shown to occur in transformed cell lines, and to modify less than 10 % of enolase molecules [43].

Our data, obtained by CPB treatment of the pure mouse β-enolase and the addition of a specific inhibitor of basic carboxypeptidases during extraction, support the hypothesis that the two major variants of the mouse β-enolase subunit differ by the presence or absence of a C-terminal lysine. Both known basic carboxypeptidases, N and B, are quite similar regarding their physiological role; they are important in regulating the circulating levels of pro-inflammatory peptides such as bradykinin and anaphylatoxins [44]. The existence of an intracellular basic carboxypeptidase has now been described [45]. It has been shown recently that plasma carboxypeptidase N and CPB are both capable of significantly reducing plasminogen binding to cells and can control the rate of cell-associated proteolysis [46]. Thus an endogenous carboxypeptidase could regulate the binding capacity of the β-enolase subunit to plasminogen, and of the α subunit as well.

Selective binding properties of enolase isoforms and a possible functional role

We have shown here, using the mouse purified isoforms, that $\beta\beta$-, like $\alpha\alpha$-, and unlike $\gamma\gamma$-enolase, can bind plasminogen with high affinity. We find that the EC_{50} values (0.1 nM) for $\alpha\alpha$- and $\beta\beta$-enolase in plasminogen binding are similar. We obtained a similar result with the commercial rabbit $\beta\beta$-enolase. This value, lower than that previously reported for human $\alpha\alpha$- and rabbit $\beta\beta$-enolase (K_d 1.4–1.6 μM; [34]), clearly reflects a higher affinity for plasminogen. The difference with published results might arise from different experimental conditions, especially the use of ^{125}I-labelled plasminogen in other binding studies. Nevertheless, these results underline once more that enolase, as many other glycolytic enzymes, could have functions unrelated to glycolysis [47,48]. Interestingly, the plasminogen activation system appears to be directly involved in the fusion processes accompanying myogenic differentiation [49]. It will be important to clarify the physiological roles of both α- and β-enolase subunits during these fusion reactions.

Our binding studies demonstrate for the first time that pure

$\beta\beta$-enolase associates with high affinity with aldolase, PK and creatine kinase that have been purified from skeletal muscle. Interaction between enolase and PGM extracted from muscle tissues has previously been observed by others [50]. However, from the estimate of the dissociation constant (K_d), the binding reported by these authors is weaker than that reported by us ($K_d = 1\ \mu$M, compared with 3–8 nM found here). Furthermore, they observed a similar K_d value for the $\alpha\alpha$-, $\beta\beta$- and $\gamma\gamma$-isoenolases, whereas we do not observe high-affinity binding between the muscle PGM and the neuron-specific $\gamma\gamma$-enolase. These discrepancies might be explained by the ELISA procedure that they have used, which is completely different from ours and yields estimates of the K_d value through indirect computations.

We also show for the first time that $\beta\beta$-enolase binds the sarcomeric protein troponin. Enolase association with other enzymes and troponin appears to be stronger at acidic pH, in contrast with the association of $\beta\beta$-enolase with plasminogen, which is not influenced by pH (Table 3). Increased binding to cytoskeletal stuctures with a decrease of intracellular pH has been described for several glycolytic enzymes [37]. During activated glycolysis, when intracellular pH declines, enzyme interactions will enhance the metabolite transfer rate and thereby increase the glycolytic flux [51]. Thus our observation of a pH-modulated binding of $\beta\beta$-enolase to its adjacent enzymes in the pathway, PGM and PK, provides support to the hypothesis, put forward by others, that these three enzymes do form a functional glycolytic segment [19]. Moreover, the observed troponin binding would favour the formation of glycolytic enzyme complexes in close vicinity with the contractile apparatus. Similarly, aldolase is known to bind actin and tropomyosin [51]. Thus enolase could be associated with the sarcomere by binding aldolase, through a 'piggy-back' mechanism [51]. The $\alpha\alpha$ and $\beta\beta$ isoforms have similar binding properties for three enzymes analysed in this study; PGM, PK and MCK, but not for aldolase and troponin. These results could explain the observed striated pattern of α- and β-enolase immunoreactivity [11,18], suggesting that such associations are sufficient to localize the muscle enolase isoforms near the sarcomeric apparatus. This targeting might be modulated by the enolase isoform composition, which changes during development and with fibre type in adult muscles [9,11–13].

In conclusion, we have shown that changes in α and β subunit microheterogeneity accompany muscle maturation, at the time of secondary fibre formation, when important changes in muscle energy metabolism are likely to occur. The facts that $\alpha\alpha$ and $\beta\beta$ isoforms have different binding properties for aldolase and troponin, and that the $\gamma\gamma$ isoform does not bind any of the muscle proteins studied here, strongly supports our working hypothesis that enolase isoforms differ in their properties of interaction with cytoskeletal elements and/or other components of the cell. These specific interactions might distinguish the muscle enolase isoforms at the subcellular sites where ATP, produced through glycolysis, is most needed for contraction. These associations could be modulated by post-translational modifications. Phosphorylations are known to play an important role in regulating the glycolytic flux [20,52], partly by modifying the binding properties of enzymes. It will be important to further investigate their role in generating α- and β-enolase electrophoretic variants, using *in vitro* model systems.

We thank Dr. Martine Arrio-Dupont; Laboratoire de Biologie Physicochimique, Orsay, France) for determination of creatine kinase activities, Drs. P. Denoulet and J.-C. Larcher for helpful discussions, Dr. L. Legault-Demare for a critical reading of the manuscript, and J. P. Martin for the photographic art work. This work was supported by grants from the Centre National de la Recherche Scientifique to F.G., and from the Association Française contre les Myopathies to M. Lazar. T.M. was a recipient of Ministère de la Recherche and Fondation pour la Recherche Médicale.

REFERENCES

1 Craig, S. P., Day, I. N. M., Thompson, R. J. and Craig, I. W. (1990) Cytogenet. Cell Genet. **54**, 71–73
2 Feo, S., Oliva, D., Barbieri, G., Xu, W., Fried, M. and Giallongo, A. (1990) Genomics **6**, 192–194
3 Fletcher, L., Rider, C. C., Taylor, C. B., Adamson, E. D., Luke, B. M. and Graham, C. F. (1978) Dev. Biol. **65**, 462–475
4 Zomzely-Neurath, C. E. (1983) in Enzymes in the Nervous System, Handbook Of Neurochemistry, vol. 4 (Lajtha, A., ed.), pp. 403–433, Plenum Press, New York, NY, U.S.A.
5 Keller, A., Bérod, A., Dussaillant, M., Lamandé, N., Gros, F. and Lucas, M. (1994) J. Neurosci. Res. **38**, 493–504
6 Imamura, K. and Tanaka, T. (1972) J. Biochem. **71**, 1043–1051
7 Lebherz, H. G. and Rutter, W. J. (1969) Biochemistry **8**, 109–121
8 Popovici, T., Berwald-Netter, Y., Vibert, M., Kahn, A. and Skalka, H. (1990) FEBS Lett. **268**, 189–193
9 Keller, A., Ott, M. O., Lamandé, N., Lucas, M., Gros, F., Buckingham, M. and Lazar, M. (1992) Mech. Dev. **38**, 41–54
10 Lucas, M., Goblet, C., Keller, A., Lamandé, N., Gros, F., Whalen, R. G. and Lazar, M. (1992) Differentiation, **51**, 1–7
11 Keller, A., Rouzeau, J. D., Farhadian, F., Wisniewsky, C., Marotte, F., Lamandé, N., Samuel, J. L., Schwartz, K., Lazar, M. and Lucas, M. (1995) Am. J. Physiol. (Heart Circ. Physiol. 38) **269**, H1843–H1851
12 Ibi, T., Sahashi, K., Kato, K., Takahashi, A. and Sobue, I. (1983) Muscle Nerve **6**, 661–663
13 Kato, K., Shimizu, A., Semba, R. and Satoh, T. (1985) Biochim. Biophys. Acta **841**, 50–58
14 Keller, A., Scarna, H., Mermet, A. and Pujol, J. F. (1981) J. Neurochem. **36**, 1389–1397
15 Shimizu, A., Suzuki, F. and Kato, K. (1983) Biochim. Biophys. Acta **748**, 278–284
16 Lebioda, L. and Stec, B. (1991) Int. J. Biol. Macromol. **13**, 97–100
17 Duquerroy, S., Camus, C. and Janin, J. (1995) Biochemistry **34**, 12513–12523
18 Dölken, G., Leisner, E. and Pette, D. (1975) Histochemistry **43**, 113–121
19 Masters, C. (1992) Int. J. Biochem. **24**, 405–410
20 Korge, P. and Campbell, K. B. (1995) Int. J. Sports Med. **16**, 172–179
21 Chen-Zion, M., Livnat, T. and Beitner, R. (1992) Int. J. Biochem. **24**, 821–826
22 Wegmann, G., Zanolla, E., Eppenberger, H. M. and Wallimann, T. (1992) J. Muscle Res. Cell Motil. **13**, 420–435
23 Lamandé, N., Mazo, A. M., Lucas, M., Montarras, D., Pinset, C., Gros, F., Legault-Demare, L. and Lazar, M. (1989) Proc. Natl. Acad. Sci. U.S.A. **86**, 4445–4449
24 Bradford, M. M. (1976) Anal. Biochem. **72**, 248–254
25 Harlow, E. and Lane, D. (1988) Antibodies, A Laboratory Manual, p. 125, Cold Spring Harbor Laboratory, Cold Spring Harbor, NY
26 Larcher, J. C., Boucher, D., Ginzburg, I., Gros, F. and Denoulet, P. (1992) Dev. Biol. **154**, 195–204
27 Morissey, M. (1981) Anal. Biochem. **117**, 307–310
28 Hendricks, D., Soons, J., Sharpé, S., Wevers, R., van Sande, M. and Holmquist, B. (1988) Clin. Chim. Acta **172**, 253–260
29 Plummer, T. H. and Ryan, T. J. (1981) Biochem. Biophys. Res. Commun. **98**, 448–454
30 Dessen, P., Fondrat, C., Valencien, C. and Mugnier, C. (1990) Comput. Appl. Biosci. **6**, 355–356
31 Rosenberg, U. B., Eppenberger, H. M. and Perriard, J.-C. (1981) Eur. J. Biochem. **116**, 87–92
32 Lamandé, N., Brosset, S., Lucas, M., Keller, A., Rouzeau, J.-D., Johnson, T. R., Gros, F., Ilan, J. and Lazar, M. (1995) Mol. Reprod. Dev. **41**, 306–313
33 Miles, L. A., Dahlberg, C. M., Plescia, J., Felez, J., Kato, K. and Plow, E. F. (1991) Biochemistry **30**, 1682–1691
34 Redlitz, A., Fowler, B. J., Plow, E. F. and Miles, L. A. (1995) Eur. J. Biochem. **227**, 407–415
35 Nakajima, K., Hamanoue, M., Takemoto, N., Hattori, T., Kato, K. and Kohsaka, S. (1994) J. Neurochem. **63**, 2048–2057
36 Knull, H. R. and Walsh, J. L. (1992) Curr. Top. Cell. Regul. **33**, 15–30
37 Shearwin, K. and Masters, C. (1990) Biochem. Int. **22**, 735–740
38 Asaga, H. and Konno, K. (1975) J. Biochem. (Tokyo) **77**, 867–877
39 Cardenas, J. M. and Wold, F. (1971) Arch. Biochem. Biophys. **144**, 663–672
40 Bottalico, L., Kendrick, N., Keller, A., Li, Y. and Tabas, I. (1993) Arterioscler. Thromb. **13**, 264–275
41 Oliva, D., Venturella, S., Passantino, R., Feo, S. and Giallongo, A. (1995) Eur. J. Biochem. **232**, 141–149
42 Nettelblad, F. A. and Engström, L. (1987) FEBS Lett. **214**, 249–252
43 Cooper, J. A., Esch, F. S., Taylor, S. S. and Hunter, T. (1984) J. Biol. Chem. **259**, 7835–7841

44 Skidgel, R. A. (1995) Methods Enzymol. **248**, 653–663
45 Ohkubo, K., Okuda, M. and Kaliner, M. (1994) Rhinology **31**, 130–133
46 Redlitz, A., Tan, A. K., Eaton, D. L. and Plow, E. F. (1995) J. Clin. Invest. **96**, 2534–2538
47 Takei, N., Kondo, J., Nagaike, K., Ohsawa, K., Kato, K. and Kohsaka, S. (1991) J. Neurochem. **57**, 1178–1184
48 Kim, R., Lietman, T., Piatigorsky, J. and Wistow, G. (1991) Gene **103**, 193–200
49 Quax, P. H. A., Frisdal, E., Pedersen, N., Bonavaud, S., Thibert, P., Martelly, I., Verheijen, J. H., Blasi, F. and Barlovatz-Meimon, G. (1992) Dev. Biol. **151**, 166–175
50 Nazarian, K. B., Climent, F., Simonian, S., Tompa, P. and Batke, J. (1992) Arch. Biochem. Biophys. **296**, 650–653
51 Clarke, F., Stephan, P., Morton, D. and Weidemann, J. (1985) in Regulation of Carbohydrate Metabolism, vol. 2 (Beitner, R., ed.), pp. 1–31, CRC Press, Boca Raton
52 Storey, K. B. (1985) Mol. Physiol. **8**, 439–461

Received 10 October 1996/9 December 1996; accepted 6 January 1997